

Numerical Simulation of Buffer Flow in a Free Flow Electrophoresis Chamber

By

Hiromi YAMAGUCHI*, Masahiro ISHII*, Kazuo UEMATSU*,
Hiroyuki UCHIDA*, Sintaro ENYA* and Hisao AZUMA**

(May 1, 1990)

Summary: Free flow electrophoresis facilities used for the refining of biological materials such as blood and protein are limited in their performance by the disturbance of buffer flow. Two types of convection which cause the flow disturbance in an electrophoresis chamber were studied. Numerical investigation on natural convection by Joule heat has proved that the flow field in the electrophoretic chamber is characterized by the Reynolds, the Grashof and the Prandtl numbers. It also has been found the critical condition where the convective flow arises is presented by a relationship between the Reynolds and the Grashof numbers. Electroosmotic convection combined with the natural one in a three-dimensional model was calculated. Horizontal and vertical flow are not individually conserved in their flux because a complex three-dimensional flow pattern is formed.

1. INTRODUCTION

Electrophoresis is a biological method to separate and purify materials by the difference of the electric mobility of each particle in electric field. Among the electrophoresis methods, a free flow type, which facilitates continuous retrieval of individual ingredients, is most likely used. The efficient operation of the free flow electrophoresis facilities requires that each ingredient moves depending only on its electric mobility. However, the disturbance of buffer flow and the diffusion of samples limit the performance of the facilities.

The disturbance of buffer flow is mainly caused by two types of convection; one is natural and the other is electroosmotic one. Natural convection is raised by the interaction between Joule heat and gravity. Chamber walls are cooled down in order to protect biological samples from Joule heat, and stationary temperature gradient is established. Natural convection is enhanced by this cooling effect as shown in Fig. 1. On the other hand, electroosmotic convection is attributed to electric potential gap between the electrically-insulated walls and fluid. The potential gap forms electric double layers which move along the walls by electrostatic force and result in convection in a horizontal plane.

Since natural convection can be removed under the reduced gravity, electrophoresis experiments in space have been conducted to improve the performance of the facilities [1][2][3]. However, the critical conditions under which these convections

* Ishikawajima-Harima Heavy Industries Co., Ltd. 1, Shin-nakahara-cho, Isogo-ku, Yokohama 235, Japan

** National Aerospace Laboratory 7-44-1, Jindaiji Higashi-cho, Chyofu-shi, Tokyo 182, Japan

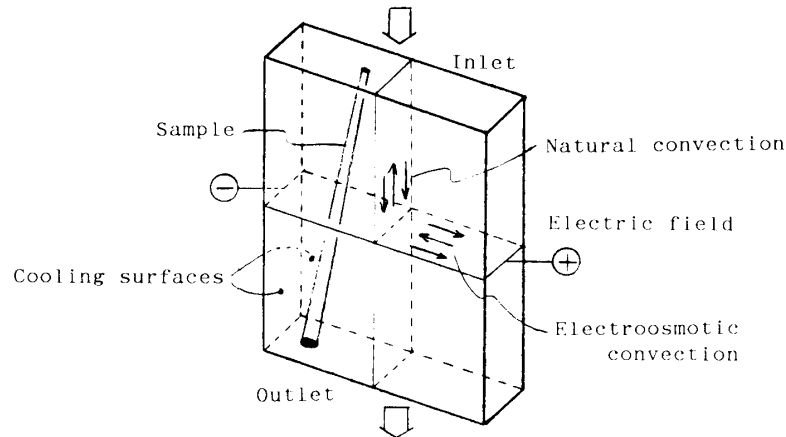


Fig. 1. Electrophoresis chamber.

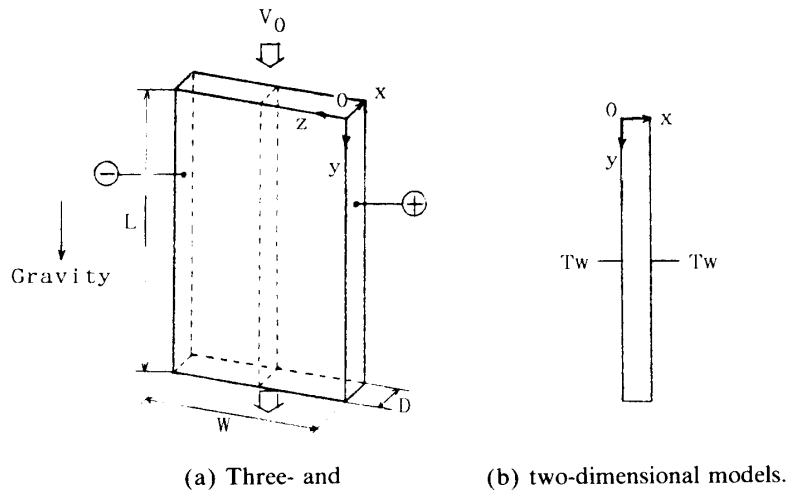


Fig. 2. Calculation models

occur remain to lack in the mature consideration.

Numerical investigation on a buffer flow in an electrophoresis chamber was carried out to discuss usefulness of space experiments by means of; (a) clarifying the critical point where the flow disturbance caused by natural convection arises and (b) estimating a three-dimensional combination flow of natural and electroosmotic convections.

2. GOVERNING EQUATIONS AND CALCULATION CONDITIONS

2-1. Calculation model

Figure 2 shows a narrow rectangular chamber for the present calculation. Fluid enters through the top surface ($y=0$) at a constant velocity, and goes out through the bottom ($y=L$) without velocity gradient. Two walls at $Z=0$ and W are electrodes, while two walls at $X=0$ and D perpendicular to the electrodes are

electrically-insulated. The insulated walls are cooled at constant temperature ($= T_w$) to suppress the temperature increase due to Joule heat. The temperature dependence of fluid properties can be neglected since the temperature difference in the chamber is a few degrees at most.

2-2. Equations and Boundary Conditions

We have considered a steady incompressible viscous flow, supposing physiological solution, in a two-dimensional model as shown in Fig. 2(b). Governing equations are given by

$$\nabla \cdot \mathbf{u} = 0 \quad (1)$$

$$(\mathbf{u} \cdot \nabla) \mathbf{u} = -\frac{1}{\rho} \nabla p + \nu \Delta \mathbf{u} + G\beta(T - T_w) \mathbf{e}_y \quad (2)$$

$$(\mathbf{u} \cdot \nabla) T = \frac{\lambda}{\rho C_p} \Delta T + \frac{\sigma E^2}{\rho C_p} \quad (3)$$

where \mathbf{u} represents velocity vector of buffer flow, p pressure, T temperature, ρ density, ν kinematic viscosity, G the gravitational acceleration, β thermal expansion coefficient, \mathbf{e}_y a unit vector along the y -axis and λ , C_p , σ and E are thermal conductivity, specific heat at constant volume, electrical conductivity and the intensity of electric field, respectively. Equations (1), (2) and (3) imply the conservation of mass, momentum and energy, respectively. Equation(2) includes a term of Boussinesq approximated buoyancy on its right hand. The second term of on the right-hand side of Eq.(3) expresses Joule heat.

Boundary conditions are stated on the cooling walls, the top surface and the bottom surface as

$$\mathbf{u} = (0, 0), \quad T = T_w \quad \text{at } x=0, D, \quad (4)$$

$$\mathbf{u} = (0, v_0), \quad T = T_w \quad \text{at } y=0, \quad (5)$$

$$\frac{\partial \mathbf{u}}{\partial y} = 0, \quad \frac{\partial T}{\partial y} = 0 \quad \text{at } y=L, \quad (6)$$

where v_0 is the inlet velocity of buffer fluid.

These equations are rewritten in nondimensional forms introducing non-dimensional variables denoted by tildes as

$$\tilde{x} = x/D, \quad (7)$$

$$\tilde{\mathbf{u}} = \mathbf{u}/v_0, \quad (8)$$

$$\tilde{p} = p/\rho v_0^2, \quad (9)$$

$$\tilde{T} = (T - T_w)/(T_f - T_w), \quad (10)$$

where T_f is the reference temperature of buffer fluid at the center of the chamber when all heat is carried by thermal conduction, defined as

$$T_f - T_w = \frac{\sigma E^2 D^2}{8\lambda}, \quad (11)$$

The governing equations and the boundary conditions become

$$\nabla \cdot \tilde{\mathbf{u}} = 0, \quad (12)$$

$$(\tilde{\mathbf{u}} \cdot \nabla) \tilde{\mathbf{u}} = -\nabla \tilde{p} + \frac{1}{Re} \Delta \tilde{\mathbf{u}} + \frac{Gr}{Re^2} \tilde{T} \mathbf{e}_y, \quad (13)$$

$$(\tilde{\mathbf{u}} \cdot \nabla) \tilde{T} = \frac{1}{Re Pr} \Delta T + \frac{1}{8 Re Pr}, \quad (14)$$

$$\tilde{\mathbf{u}} = (0, 0) \quad \text{at} \quad \tilde{x} = 0, 1, \quad (15)$$

$$\tilde{\mathbf{u}} = (0, 1) \quad \text{at} \quad \tilde{y} = 0, \quad (16)$$

$$\frac{\partial \tilde{\mathbf{u}}}{\partial \tilde{y}} = 0, \quad \frac{\partial \tilde{T}}{\partial \tilde{y}} = 0 \quad \text{at} \quad \tilde{y} = \frac{L}{D}, \quad (17)$$

where

$$Re = \frac{D v_0}{\nu}, \quad (18)$$

$$Pr = \frac{\rho C_p \nu}{\lambda}, \quad (19)$$

$$Gr = \frac{G \beta (T_f - T_w) D^3}{\nu^2}. \quad (20)$$

The system of the above equations are solved with a upwind differencing method using the general analysis code PHOENICS [4].

3. NUMERICAL RESULTS AND DISCUSSION

A free flow electrophoresis facility is usually operated at the inlet velocity of about 1 mm/s in a chamber of a few mm or less in depth. Physiological solution diluted to about 0.01M is used as buffer fluid. Representative values of the properties of buffer fluid and operation conditions are shown in Table 1. We obtained nondimensional parameters from these values. Figure 3 shows calculation results. Natural convection disappears as the Grashof number decreases. Counter flow caused by natural convection gives rise to the flow disturbance and then the lowering of the facility performance. We have defined the critical Grashof number (Gr_{cr}) as the Grashof number where counter flow vanishes entirely in the chamber when decreasing the Grashof number at the fixed Reynolds and Prandtl numbers.

Figure 4 represents Gr_{cr} versus the Reynolds number with the Prandtl number as a parameter. It is found that Gr_{cr} is 140 Re and is independent of the Prandtl number. In other words, the vertical flow can be characterized by two parameters

Table 1 Properties of buffer fluid and operation conditions

Density	$\rho = 1.0 \times 10^3 \text{ kg/m}^3$
Kinematic viscosity	$\nu = 1.0 \times 10^{-6} \text{ m}^2$
Coefficient of expansion	$\beta = 2.1 \times 10^{-4} / \text{K}$
Specific heat at constant volume	$C_p = 4.18 \times 10^3 \text{ J/kg/K}$
Thermal conductivity	$\lambda = 0.588 \text{ W/m/K}$
Electrical conductivity	$\sigma = 1.0 \times 10^{-2} / \Omega/\text{m}$
Wall temperature	$T_w = 20^\circ \text{C}$

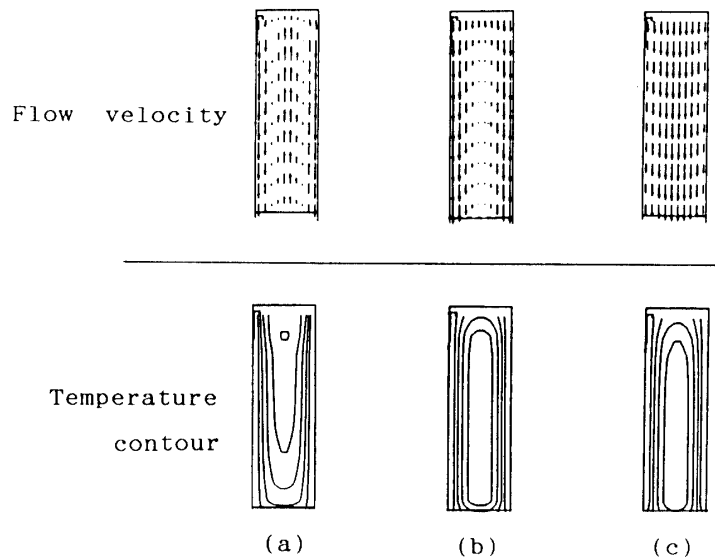


Fig. 3. Variation of flow velocity and temperature distribution at $Re=5$, $Pr=7$ and $Gr=(a) 1400$, $(b) 700$ and $(c) 1.4$.

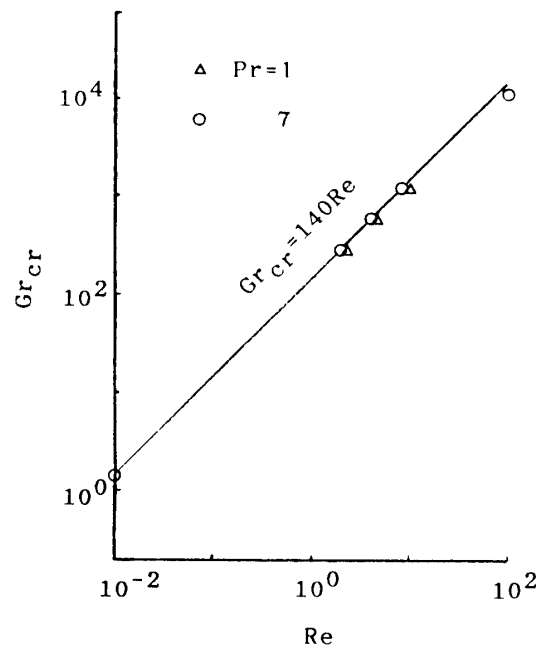


Fig. 4. Correlation of 'critical' Grashof number to Reynolds number.

of Re and Gr in the narrow rectangular chamber in which gravity works perpendicular to the temperature gradient. In Fig. 4, natural convection is dominant in the region above the critical line of $Gr_{cr}=140Re$, while forced transport determines the flow pattern in the region below the critical line. When the buffer fluid comes in at the velocity of 1 mm/s to a chamber of 5 mm thickness, the critical Grashoff number becomes 700, for example, which corresponds to about 0.5G with $1W/cm^3$ internal heating. This example suggests that this equipment must be operated under less than 0.5G.

Since both Re and Gr are increasing in proportion to third power of the chamber thickness D , the increase of D enhances natural convection more sensitively than that of gravity and of temperature difference term $(T_f - T_w)$. On the contrary, the decrease of D reduces quantity of sample retrieval. Therefore the chamber of about 1mm thickness is considered to be a limit size for an experiment on the ground. The breakthrough of this limitation requires the operation under the micro-gravity condition in order to increase quantity and fineness of samples.

4. ELECTROOSMOSIS

4-1. Calculation Model

Furthermore we simulate electroosmotic flow combined with natural convection in a three dimensional model as shown in Fig. 2(a). Electroosmotic velocity V_{eo} is introduced to represent the magnitude of electroosmotic effect.

$$V_{eo} = \frac{\varepsilon E \zeta}{\mu} \quad (21)$$

where ε is dielectric constant of the solution, ζ is the difference of zeta potential between the chamber wall and fluid and μ is fluid viscosity. Decrement of V_{eo} is effective to suppress electroosmotic convection. However, the smaller dielectric constant leads to the larger electrical conductivity and then to the increase of Joule heat. Weak electric field intensity reduces the precision of sample separation. Viscosity is almost the same as that of water, for buffer solution almost consists of water. Thus it is the most convenient to control zeta potential by selecting wall materials which have small potential gap to the fluid. It has been reported [8] that zeta potential is reduced to several mV by appropriate surface coating on the wall. For example, when E and ζ equal to 100 V/cm and 1 mV respectively, V_{eo} is evaluated to be 0.01 mm/s. We analyzed how convection pattern changed under micro- and one gravity conditions when V_{eo} is 0.01 and 1 mm/s. Here we assumed micro-G to be $10^{-4}G$ corresponding to the space station's condition. Electroosmotic effect is given as a boundary condition;

$$\mathbf{u} = (0, 0, V_{eo}) \quad \text{at } x=0, D, \quad (22)$$

which implies that electrically-insulated walls move without slip to fluid.

4-2. Results and Discussion

Figure 5 shows electroosmotic and natural convection patterns and streamlines from the inlet to the outlet of the chamber. Electroosmotic convection can be seen on a horizontal plane. When V_{eo} is 0.01 mm/s, horizontal convection is very small compared with vertical flow. But this small convection cannot be neglected because it leads to the sample drift of a few mm during the sample moves from the top surface to the bottom. This drift caused by electroosmotic convection limits the precision of the sample separation.

The detailed horizontal flow velocity distribution is shown in Fig. 6. The difference of velocity profiles at 1G and micro-G is small. But it is shown from

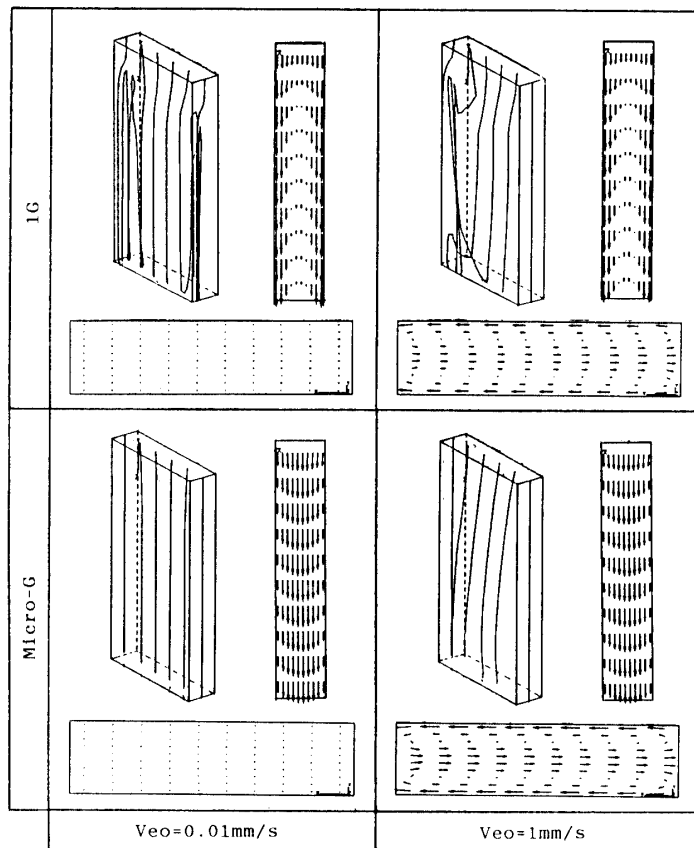


Fig. 5. Disturbance of buffer flow at $Re=5$, $Pr=7$, representing streamlines and vertical ($\hat{Z}=0.5$) and horizontal ($\hat{Y}=0.5$) velocity profiles. \hat{Y} - and \hat{Z} - axes are normalized by depth and width of the chamber, respectively.

the unbalance of integrals of $+z$ and $-z$ directional vectors indicates that the horizontal flow is not conserved in flux. This fact suggests that vertical flow influences horizontal one and then three-dimensional complex flow occurs to conserve flux as shown by streamlines in Fig. 6. This result also implies that natural and electroosmotic convections cannot be considered independently.

5. CONCLUSION

The flow in a narrow rectangular chamber with internal heat generation was applied to that in a free flow electrophoresis chamber. The present model has the features that main flow is parallel with gravity and that temperature gradient is perpendicular to gravity.

Electric field causes two types of disturbance, natural and electroosmotic convections. We have obtained the following results;

(a) We estimated the contribution of gravity, electric field intensity and chamber thickness to natural convection by introducing nondimensional parameters. It has been found that the "critical" Grashof number Gr_{cr} , at which counter flow caused by natural convection arises and/or disappears, depends only upon the Reynolds number. This Gr_{cr} gives a critical point to design an electrophoresis

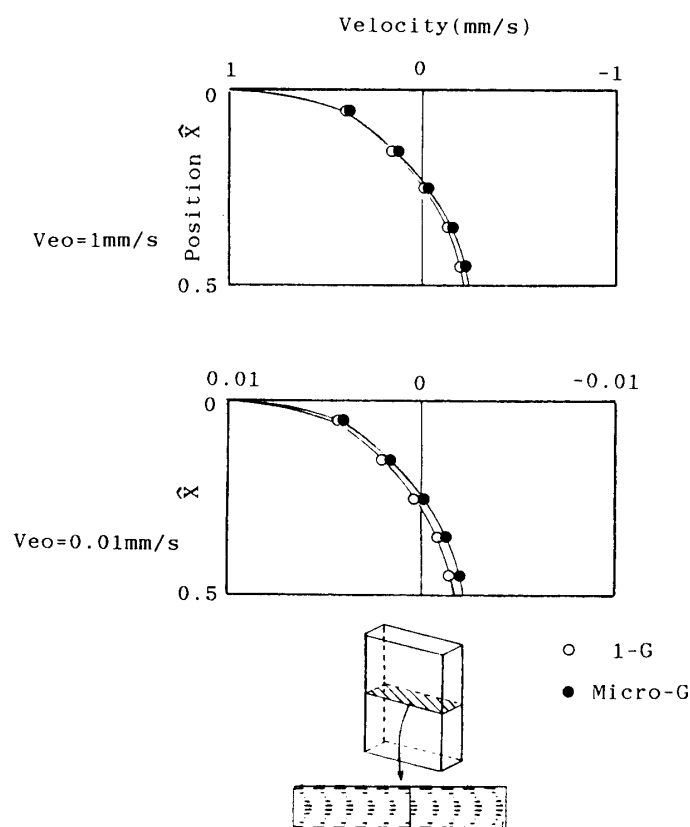


Fig. 6. Distribution of electroosmotic flow velocity at $\hat{Z}=0.5$ on a horizontal plane ($\hat{Y}=0.5$) as shown in the below part.

chamber in which the flow disturbance due to natural convection does not occur.

(b) Electroosmosis gives rise to horizontal convection along the electric field. Electroosmotic convection makes it hard to separate ingredients within 1 mm positional accuracy even if $V_{eo}=0.01$ mm/s. The combination of natural and electroosmotic convections results in three-dimensional complex flow. The precise electroosmotic effect must be estimated taking natural convection into account.

These results are helpful for an understanding of the buffer flow and an optimum design of electrophoresis chamber. The performance of electrophoresis facilities is improved under micro-gravity condition and electroosmotic effect which limits the precision of sample retrieval cannot be neglected even if such walls as provide small zeta-potential are used.

REFERENCES

- [1] E. C. McKannan, et al., NASA TMX-64611, 1971
- [2] J. W. Vanderhoff, et al., NASA CP-149925, 1976
- [3] V. Mang, Appl. Microgravity Tech. Vol. 1, pp. 52-56, 1989
- [4] S. U. Patankar, 'Numerical Heat Transfer and Fluid Flow', Hemisphere Publishing Co., 1980
- [5] S. Nagaoka, et al., Proceedings of 16th ISTS, pp. 2465-2470, Sapporo, 1988
- [6] D. A. Saville, S. Ostrach, NASA CR-150689, 1978
- [7] T. W. Nee, J. Chromatography, Vol. 105, pp. 231-249, 1975
- [8] T. Adachi, et al., J. Jap. Soc. Microgravity Appl. Vol. 5, No. 3, pp. 31-33, 1988